AD-A032 848 NAVAL RESEARCH LAB WASHINGTON D C F/G 7/4
I* ATOM BIMOLECULAR QUENCHING BY O2, H2O, H2O2, AND H2.(U)
OCT 76 J R MCDONALD, J K HANCOCK
UNCLASSIFIED NRL-MR-3395 NL

| OF |
AD
A032 848

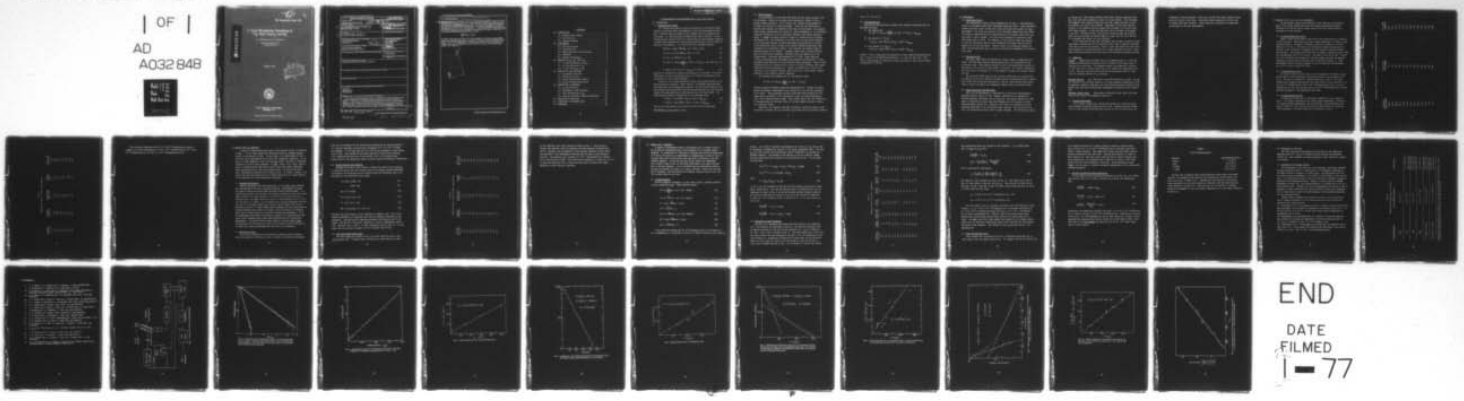

END
DATE
FILMED
1-77

NRL Memorandum Report 3395

I* Atom Bimolecular Quenching by O_2, H_2O, H_2O_2, and H_2

J. R. McDonald and J. K. Hancock

Physical Chemistry Branch
Chemistry Division

October 1976

NAVAL RESEARCH LABORATORY
Washington, D.C.

SECURITY CLASSIFICATION OF THIS PAGE (When Data Entered)

REPORT DOCUMENTATION PAGE

READ INSTRUCTIONS BEFORE COMPLETING FORM

1. REPORT NUMBER: NRL Memorandum Report 3395 (14)	2. GOVT ACCESSION NO.: NRL-MR-3395
3. RECIPIENT'S CATALOG NUMBER	
4. TITLE (and Subtitle): (6) I* ATOM BIMOLECULAR QUENCHING BY O_2, H_2O, H_2O_2, AND H_2.	5. TYPE OF REPORT & PERIOD COVERED: (9) Final report, Feb[illegible]–Jun[illegible]75
	6. PERFORMING ORG. REPORT NUMBER
7. AUTHOR(s): (10) J. R. McDonald [illegible] J. K. Hancock	8. CONTRACT OR GRANT NUMBER(s)
9. PERFORMING ORGANIZATION NAME AND ADDRESS: Naval Research Laboratory, Washington, D.C. (12) 30p.	10. PROGRAM ELEMENT, PROJECT, TASK AREA & WORK UNIT NUMBERS: NRL Problem C07-01, AFWL 75-265
11. CONTROLLING OFFICE NAME AND ADDRESS: Air Force Weapons Laboratory, Kirtland AFB, New Mexico 87117 (11)	12. REPORT DATE: Oct[illegible]976
	13. NUMBER OF PAGES: 37
14. MONITORING AGENCY NAME & ADDRESS(if different from Controlling Office)	15. SECURITY CLASS. (of this report): UNCLASSIFIED
	15a. DECLASSIFICATION/DOWNGRADING SCHEDULE

16. DISTRIBUTION STATEMENT (of this Report)
Approved for public release; distribution unlimited.

17. DISTRIBUTION STATEMENT (of the abstract entered in Block 20, if different from Report)

18. SUPPLEMENTARY NOTES

19. KEY WORDS (Continue on reverse side if necessary and identify by block number)
Iodine atom
Quenching rates
Chemical laser

20. ABSTRACT (Continue on reverse side if necessary and identify by block number)

Iodine atom quenching rates in the presence of n-C_3F_7I, H_2, O_2, H_2O and H_2O_2 have been measured. Electronically excited $I(^2P_{1/2})$ atoms were produced by laser photodissociation of n-C_3F_7I at ~ 2985A using a frequency doubled flashlamp pumped dye laser. The concentration of $I(^2P_{1/2})$ is directly monitored by observing 1.315 μm fluorescence, using a liquid N_2 cooled Ge photovoltaic detector. Fluorescence signals were digitized and signal averaged using a Biomation 8100 - Nicolet 1074 transient recorder - signal averager combination. Simple biomolecular quenching

→ next page

(Continues)

DD FORM 1 JAN 73 1473 EDITION OF 1 NOV 65 IS OBSOLETE S/N 0102-014-6601

SECURITY CLASSIFICATION OF THIS PAGE (When Data Entered)

approximately

micrometer

*(2)P(1/2)

251 950

20. Abstract (Continued)

rates were measured for n-C_3F_7I ($k < 2.5 \times 10^{-15}$ cm^3/molecule·sec), H_2 ($k = 0.83 \times 10^{-13}$ cm^3/molecule·sec), and H_2O_2 ($k = 3.75 \times 10^{-12}$ cm^3/molecule·sec). Both I*-O_2 and I*-H_2O_2 mixtures exhibit strongly nonexponential fluorescence decays. The I*-H_2O_2 results suggest that both reactive and collisional quenching processes are taking place. The fast process corresponds to an apparent quenching rate of $k = 4.0 \times 10^{-11}$ cm^3/molecule·sec. A double exponential fluorescence decay from I*-O_2 mixtures suggests that two rate equations must be considered to explain our observations. The first of these if E-E pumping mechanism $I(^2P_{1/2}) + O_2(^3\Sigma)$

$$\underset{k_e'}{\overset{k_e}{\rightleftharpoons}} I(^2P_{3/2}) + O_2(^1\Delta)$$

for which we find a rate of $k_e = 0.96 \times 10^{-11}$ cm^3/molecule·sec. The other rate most probably represents an irreversible energy sink for I populations. Several mechanisms are investigated for this rate $k = 1.42 \times 10^{-11}$ cm^3/molecule·sec. A major kinetic analysis is carried out based upon the assumption that the rate corresponds to the E-VT process k_{12}, $I(^2P_{1/2}) + O_2(^3\Sigma) \xrightarrow{k_{12}} I(^2P_{3/2}) + O_2(^3\Sigma) + \Delta E = 7606$ cm^{-1}.

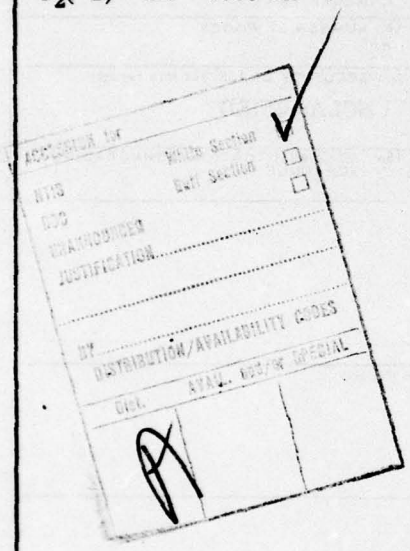

CONTENTS

I* ATOM BIMOLECULAR QUENCHING BY O_2, H_2O, H_2O_2, AND H_2

1.0 INTRODUCTION

1.1 Chemical Laser Scheme

A cw iodine atom chemical laser with potential for high power applications is presently under investigation at the Air Force Weapons Laboratory. Several potential chemical laser schemes have been suggested and considered. I_2, which quenches the upper laser state, $I(^2P_{1/2})$, at near the gas kinetic collision rate [1], renders many of these schemes untenable. A scheme which minimizes this quenching process has been chosen by AFWL for extensive investigation. It is based upon the following sequence:

$$Ca(ClO)_2 + 2H_2O_2 \xrightarrow{k_1} 2O_2\ (^1\Delta) + 2H_2O + CaCl_2 \quad (1)$$

$$O_2\ (^1\Delta) + O_2\ (^1\Delta) \xrightarrow{k_2} O_2\ (^1\Sigma) + O_2\ (^3\Sigma) \quad (2)$$

$$O_2\ (^1\Sigma) + I_2 \xrightarrow{k_3} 2I + O_2\ (^3\Sigma) \quad (3)$$

$$O_2\ (^1\Delta) + I\ (^2P_{3/2}) \underset{k_{-4}}{\overset{k_4}{\rightleftharpoons}} O_2\ (^3\Sigma) + I\ (^2P_{1/2}) + \Delta E = 280\ cm^{-1} \quad (4)$$

$$I\ (^2P_{1/2}) \longrightarrow I\ (^2P_{3/2}) + h\nu_{laser}\ (1.315\ um) \quad (5)$$

Reaction (3) effectively prevents the buildup of I_2 molecules. The $O_2(^1\Sigma)$ responsible for this dissociation occurs as a natural consequence of the deactivation of O_2 by self-quenching.

Pursuit of this scheme introduces further uncertainaties which it has been necessary to consider. These include: (1) Reagent mixing problems associated with the heterogeneous reaction; (2) The resultant need to separate aerosols and particulates from the reaction mixture; and (3) The introduction of large quantities of H_2O and H_2O_2 into the laser medium. The later process requires consideration of the following rates;

$$I\ (^2P_{1/2}) + H_2O \xrightarrow{k_6} I\ (^2P_{3/2}) + H_2O\dagger + \Delta E_{trans} \quad (6)$$

$$I\ (^2P_{1/2}) + H_2O_2 \xrightarrow{k_7} I\ (^2P_{3/2}) + H_2O_2\dagger + \Delta E_{trans} \quad (7)$$

Rate k_7 may also include collisionally induced reactive mechanisms.

Note: Manuscript submitted September 30, 1976.

1.2 Rate Constants

At the inception of this work firm values for the rates k_6 and k_7 were not available. Husain and coworkers have extensively studied I ($^2P_{1/2}$) energy transfer kinetics. In all studies the initial concentrations of I* atoms are produced by flash photolysis. Detection and monitoring of excited state species are primarily based upon two techniques; (a) secondary flash kinetic spectroscopy and vacuum u.v. plate photometry; or (b) following transient absorption by use of resonance radiation from iodine resonance lamps. A summary of these studies is found in a review article by Husain and Donovan [2]. The evaluation of the fast rates by the latter technique is more uncertain because in these experiments the monitoring of excited state populations does not begin until several hundred microseconds after initiation of the photolysis pulse. This restricts the dynamic range of pressures which can be studied. Lifetimes longer than a few milliseconds must be corrected for diffusion, radiative decay and impurities in the diluent gases. McFarlane and coworkers [3], in 1974, began reporting I ($^2P_{1/2}$) quenching rates following laser photolysis of precursors. I atom populations were monitored by time resolved atomic absorption. Some of these quenching rates were reported to be a factor of twenty different from values reported by Deakin and Husain [4]. Similar uncertainties in crucial rate constants in the proposed chemical iodine atom laser, would render computer modeling of this system a useless endeavour.

The essential E-E pumping step for the chemical laser,

$$O_2\ (^1\Delta) + I\ (^2P_{3/2}) \underset{k_{-4}}{\overset{k_4}{\rightleftharpoons}} O_2\ (^3\Sigma) + I\ (^2P_{1/2})$$

has been studied by Deakin, Husain and Wiesenfield [4]. Because of experimental constraints, measurements were carried out at O_2 and CF_3I pressures of 2-6 mtorr. These pressures are much lower than those required for the laser device; moreover, it was necessary to carry out these measurements over a very limited pressure range. Some concern exists over the feasibility of extrapolating the evaluated rates to the much higher pressures required in a practical device.

Therefore, with support from AFWL the Physical Chemistry Branch at NRL undertook to measure the rate constants associated with the processes detailed

in Eq. (4), (6) and (7).

1.3 Proposed Research

Specifically NRL undertook to measure rate constants associated with the following processes:

1) The pumping step

$$O_2\ (^1\Delta) + I\ (^2P_{3/2}) \underset{k_{-4}}{\overset{k_4}{\rightleftharpoons}} O_2\ (^3\Sigma) + I\ (^2P_{1/2}) + \Delta E_{trans}$$

2) H_2O removal of I ($^2P_{1/2}$)

$$I\ (^2P_{1/2}) + H_2O \xrightarrow{k_6} I\ (^2P_{3/2}) + H_2O^{\ddagger} + \Delta E_{trans}$$

3) H_2O_2 removal of I ($^2P_{1/2}$)

$$I\ (^2P_{1/2}) + H_2O_2 \xrightarrow{k_7} I\ (^2P_{3/2}) + H_2O_2^{\ddagger} + \Delta E_{trans}$$

Initial I ($^2P_{1/2}$) populations are generated by laser induced photodissociation ($\Delta t \leq 1$ μsec) of the appropriate precursor, i.e. C_3F_7I or CF_3I, etc. The I ($^2P_{1/2}$) concentration is monitored by direct detection of time resolved atomic fluorescence at 1.315 μm.

2.0 EXPERIMENTAL

2.1 Photolysis Source

The experimental setup is shown schematically in Fig. 1. The photolysis source is a Chromatix Model CMX-4 flashlamp pumped dye laser. After evaluating several photolysis laser sources this setup was deemed most useful for these experiments. The laser was operated in the frequency doubled mode near 2985Å. The system as operating here is characterized by ~0.3 mjoule pulses which are just under 1 μsec in length. The laser can be operated at repetition rates from single shot to 30 Hz. For purposes of this work the laser was operated at very low repetition rates to allow diffusion of products from the active region prior to the next pulse. Various lenses can be employed between the laser and the photolysis cell to control the waist and divergence of the photolysis beam.

2.2 Photolysis Cell

The laser light enters the photolysis cuvette which is externally mirrored. The cell when properly adjusted gives rise to 10 traversals of the excitation laser. When tightly focused the first reflecting mirror surface is destroyed by the photolysis laser within a few shots. For typical experiments the laser beam is columnated at ~1.5 mm diameter and makes 6-10 passes through the cell.

The scattered 2985Å light and any spurious fluorescence is isolated from the detector by use of a Corning 7-56 glass filter in combination with a dielectric filter with a band pass centered at 1.315 μm. These filters were sufficient to reduce the empty cell background signals below the detection limit.

2.3 Signal Detection and Processing

The 1.315 μm fluorescence is monitored by an intrinsic photoconductive germuium detector cooled to 77°K. Signals, amplified by an impedencence matched amplifier associated with the detector, are further enhanced by a PAR model 113 amplifier in which some high frequency and low frequency rolloff smoothing maybe carried out. Signals at this point are adequate for photographing single-shot on an oscilloscope when required. More typically, however, the fluorescence decay curve is signal averaged. The fluorescence signal

is recorded by a 1000 channel Biomation model 8100 transient digitizer which has a time resolution increment as small as 10 nsec/channel. This instrument "pretriggers" fifty channels before the real time trigger and hence records the complete rise time of the waveform. Subsequent to each laser shot the contents of the Biomation 8100 are dumped into the memory of a Nicolet model 1074 signal averager. In this way many shots can be averaged in the memory of the 1074. The decay curves, corrected for scattered light and baseline drift are then available as digital signals on paper tape for curve fitting or as analogue hard copies on a chart recorder.

It was discovered during early experiments that buildup of products during long signal averaging even at low repetition rates leads to spurious quenching rates which could not be tolerated. Hence, no more than sixty-four laser shots were averaged at low repetition rates for a single filling of the cell. Under these operating conditions the decay curves were uneffected by product buildup.

2.4 Chemicals

n-C_3F_7I Commercially available C_3F_7I is contaminated with I_2. Very slow vacuum distillation from chloroform (-64°C) or nonane (-54°C) slush baths is required for purification. The compound becomes recontaminated on exposure to room light and is usually redistilled on the vacuum line immediately prior to use. Even with these precautions most decay measurements made on "pure" C_3F_7I are somewhat effected by I_2 quenching.

Hydrogen Peroxide H_2O_2 (98% purity) from FMC Corporation was used. Storage and handling of the peroxide allowed it to become somewhat contaminated by H_2O. By pumping on samples of H_2O_2/H_2O, the liquid fraction becomes enriched in H_2O_2. Samples were used when freezing point measurements indicated the H_2O_2 purity > 95%.

Hydrogen, Oxygen, Argon These gases in "Research Grade" purity were used from lecture bottles from commercial suppliers.

2.5 Pressure Measurement

For all gases, except H_2O_2, pressure was measured by a Baratron capacitance monometer employing various pressure heads. Hydrogen peroxide decomposition on the pressure measuring heads was much too fast to allow their use.

Consequently, known pressures of H_2O_2 were evolved from liquid samples thermostated in various slush baths. Calibrated volume expansions were then used to obtain lower H_2O_2 pressures. These operations introduced a considerable uncertainity in the H_2O_2 measurements.

3.0 RESULTS FOR H_2, H_2O, and C_3F_7I QUENCHING

The fluorescence decay curves measured in this work are of two distinct types, clean single exponential decays and complex nonexponential decays. Quenching by O_2 and H_2O lead to decay cruves of the later type and will be considered in later sections.

3.1 I* Atom Quenching by n-C_3F_7I

Figure 1 shows typical decay curves for I* atom fluorescence as a function of C_3F_7I pressure. The decays are clearly single exponential. In Table I decay rates are given as a function of pressure; the data is presented in a Stern Volmer plot in Fig. 3. This data is of limited use because the precision of the data is not sufficient to determine the zero pressure lifetime intercept with accuracy. The purpose of this work was to attempt to measure an upper limit for the quenching rate for I* by C_3F_7I. The slope of the plot in Fig. 3 turned out to be a function of the purity of the C_3F_7I sample and hence the apparent quenching rate given here is possibly still effected by residual I_2. From measurements made on the purest samples it can be stated that the quenching rate of I* by C_3F_7I is ≤ 100 sec^{-1}/torr.

3.2 I* Atom Quenching by H_2

In order to check the consistency of our measurements with those of other workers made by other techniques, evaluation was made of the quenching of I* by H_2. The data is presented in a Stern-Volmer plot in Fig. 4. The value obtained here compares satisfactorily with other values in the literature, i.e., 0.8×10^{-13} cm^3/molecule·sec (0.85×10^{-13} cm^3/molecule·sec [5], 1.3×10^{-13} cm^3/molecule sec [6], and with the value 1.2×10^{-13} cm^3/molecule·sec [7] which appeared subsequent to the beginning of this work.

3.3 I* Atom Quenching by H_2O

A typical decay curve for I* fluorescence quenched by H_2O is shown in Fig. 5. All decays involving H_2O are cleanly single exponential - indicative of a simple quenching mechanism. The data relating to H_2O quenching is presented in Table II. Here the pressure data has been reduced for a molefraction presentation. The Stern-Volmer plot is presented in Fig. 6.

Table I

Quenching of $I(^2P_{1/2})$ Atoms Following Laser Photodissociation of n-C_3F_7I

Pressure C_3F_7I (torr)	Relaxation Time (usec)	$1/T \times 10^3$ (sec^{-1})
150.6	67	14.9
134.0	83	12.0
108.4	108	9.26
82.1	130	7.69
64.0	163	6.16
54.0	178	5.62
43.3	235	4.26
34.5	310	3.23
20.0	495	2.02
12.2	540	1.85
11.9	685	1.46
7.0	980	1.02
4.3	1220	0.82

TABLE II

Quenching of $I(^2P_{1/2})$ in $n\text{-}C_3F_7I$ - Water Mixtures

Pressure C_3F_7I (torr)	Pressure H_2O (torr)	Molefraction $X(H_2O) \times 10^{-2}$	Lifetime τ (usec)	$(p\tau)^{-1} \times 10^3$ sec^{-1} $torr^{-1}$
57.3	0	0	135	0.13
47.4	0.346	0.725	25.0	0.84
46.4	0.610	1.30	15.1	1.41
50.0	0.762	1.50	11.4	1.73
49.6	1.04	2.06	9.34	2.11
49.5	1.22	2.41	6.4	3.08
46.3	1.68	3.50	5.05	4.13
53.6	2.12	3.81	3.8	4.72

The resulting quenching rate of 3.75×10^{-12} cm^3/molecule·sec can be compared to earlier measurements of 0.94×10^{-12} cm^3/molecule·sec [8], 0.72×10^{-12} cm^3/molecule·sec [6] and 2.7×10^{-12} cm^3/molecule·sec [9].

4.0 RESULTS FOR H_2O_2 QUENCHING

A typical I^* fluorescence decay curve in the presence of H_2O_2 is presented in Fig. 7. In all cases studied the fluorescence decay is strongly nonexponential in the presence of H_2O_2. In most cases, as is demonstrated in Fig. 7, the decay can be approximated as the sum of two exponential components. In all cases, at times immediately after the photolysis pulse, the decay is completely dominated by the fast decay component, i.e. $\frac{I_s}{I_1}$ (t=0) = 5-20. Hence, experiments of limited dynamic range would appear to give near single exponential decay approximated by the fast rate measured herein. We have little faith that a biexponential analysis such as shown in Fig. 7 is unique. Indeed, it is likely that many decay processes are in effect giving rise to a decay composed of the superposition of many exponential components.

4.1 Multiphoton Processes

Several experiments were undertaken which, it was hoped, might simplify the understanding of the H_2O_2 quenching mechanism. Measurements were made with tightly focused photolysis beams and with diffuse unfocused beams. In a tightly focused beam (~0.2 mm diam.) for moderate pressures of C_3F_7I the initial number density of I^* atoms produced is ~2 x $10^{17}/cm^3$ (~6 torr) while in an unfocused beam, the number density of initial I^* atoms produced is ~2.5 x $10^{14}/cm^3$ (~10 mtorr of I atoms). In the focused case, reactive mechanisms involving H_2O_2 and I^* could easily deplete H_2O_2 from the active region, while in the unfocused condition, I^* always remains dilute compared with H_2O_2 concentrations. Strong differences were noted in the shape, relative intensity, and apparent decay rates of decay curves in the focused and unfocused experiments. Since the anticipated laser device is expected to operate at I^* concentrations near those of our unfocused limit, rates reported herein will be for unfocused measurements. It should be kept in mind, however, that much higher local concentrations of I^* and H_2O_2 are likely in any practical device, and hence it is likely that reactive mechanisms will also have to be considered.

4.2 Photolysis of H_2O_2

The relative populations of OH produced by photolysis were considered. Since the extinction coefficient of H_2O_2 is known as a function of wavelength

[10] one can determine the OH concentration produced by the laser photolysis. In a typical experiment involving H_2O_2 quenching of I*, ~1 x 10^{14} I* atoms are produced. At the same time only ~5 x 10^{10} OH are produced by light absorption of H_2O_2. Even though OH can become involved in other chain reactions (i.e. generating species such as HO_2 and HOI, etc.) it is unlikely that these result to any significant extent from the initial OH produced by photolysis.

4.3 Energy Transfer and Chemistry

Although the study of such systems is beyond the scope of this proposal, it should be pointed out that several reactive and energy transfer mechanisms are possible involving H_2O_2 and its products which may ultimately need to be considered in the modeling of this system.

$$I^* + H_2O_2 \longrightarrow HOI + OH \qquad (8)$$

$$\longrightarrow HI + HO_2 \qquad (9)$$

$$OH + I^* \longrightarrow HOI \qquad (10)$$

$$OH + H_2O_2 \longrightarrow H_2O + HO_2 \qquad (11)$$

$$I^* + HO_2 \longrightarrow I + HO_2^* \qquad (12)$$

$$HO_2 + H_2O_2 \longrightarrow H_2O + O_2 + OH, \text{ etc.} \qquad (13)$$

We would like particularly to call attention to equation (12). HO_2 is now firmly established as an important and reactive chemical constituent of the atmosphere. Both E-E and E-V quenching processes involving HO_2 and I* are likely. The HO_2 $\tilde{A} \leftarrow \tilde{A}$ electronic transition is nearly isoenergentic with I* [11]. Moreover, the ν_1 and $\nu_1 + \nu_3$ HO_2 transitions occur in the 1.0 - 2.4 μm region and are potential acceptors for E-V transfer from I* [12].

4.4 H_2O_2 Total Deactivation Rate

The Stern Volmer plot shown in Fig. 8 was made from data such as that shown in Table III. In making these evaluations an approximation was made

TABLE III

Quenching of $I(^2P_{1/2})$ Atoms in $n\text{-}C_3F_7I$ - H_2O_2 Mixtures

Pressure C_3F_7I (torr)	Pressure H_2O_2(mtorr)	Molefraction $X(H_2O_2) \times 10^{-3}$	Lifetime τ (usec)	$(p\tau)^{-1} \times 10^3$ sec^{-1} $torr^{-1}$
69.2	53	0.77	9.4	1.53
71.6	53	0.74	13	1.07
57.2	80	1.40	17	1.03
90.1	80	0.89	8.0	1.39
53.5	110	2.05	8.9	2.28
59.6	110	1.84	11.9	1.41
53.5	157	2.93	5.0	3.73
98.4	157	1.59	6.75	1.50
74.5	180	2.41	3.1	4.32
70.8	185	2.61	3.0	4.69
49.6	270	5.42	3.3	6.08
83.9	270	3.21	2.65	4.48
106.5	270	2.53	2.6	3.60

to the "apparent" fast decay process as shown in Fig. 7. This was done because this apparent rate will dominate the decay kinetics involving H_2O_2 and I^*. Moreover, our uncertainity in the absolute pressure of H_2O_2 (which was discussed in the experimental section) does not merit a more detailed analysis. The measured rate constant 4.0×10^{-11} cm^3/molecule·sec probably has an uncertainity of ±50%. This value may be compared to a value of 1×10^{-11} by Burde and McFarlane [9], in which they were able to detect only single exponential decay from H_2O_2 quenching.

5.0 RESULTS FOR O_2 QUENCHING

A typical I^* fluorescence decay in the presence of O_2 is shown in Fig. 9. In all cases I^* fluorescence decay in the presence of O_2 is strongly nonexponential. In essentially all conditions of pressure and relative concentrations of I^* and O_2 the decay can be approximated as biexponential as shown in Fig. 9. At short times after the photolysis pulse the decay is dominated by the fast lifetime component. As was the case with I^*-H_2O_2 decays, for experiments with a dynamic range of only ~10 the decay would appear to be almost entirely that of the fast component. It was concluded that the biexponential analysis for H_2O_2 was probably not unique, i.e. see eq. (8)-(13). Such is not the case for O_2 quenching. The possibilities for chemical reactions such as in eq. (8)-(13) are much fewer in this case.

5.1 O_2 Decay Kinetics

We have attempted to enumerate the most likely kinetic processes involved in the O_2 quenching scheme. These equations follow;

$$I^* + O_2 \underset{k_{e'}}{\overset{k_e}{\rightleftharpoons}} I + O_2^* + \Delta E = -280\text{cm}^{-1}, \tag{14}$$

$$I^* + O_2 \xrightarrow{k_{12}} I + O_2 + \Delta E = 7605\text{cm}^{-1}, \tag{15}$$

$$I^* + C_3F_7I \xrightarrow{k_{1m}} I + C_3F_7I, \tag{16}$$

$$I^* + I \xrightarrow{k_{11}} I + I, \tag{17}$$

$$O_2^* + O_2 \xrightarrow{k_{22}} O_2 + O_2 + \Delta E = 7885\text{cm}^{-1}, \tag{18}$$

$$O_2^* + C_3F_7I \xrightarrow{k_{2m}} O_2 + C_3F_7I, \tag{19}$$

$$O_2^* + I \xrightarrow{k_{21}} O_2 + I. \tag{20}$$

If we accept the premise that the I^* fluorescence decay in the presence of O_2 is biexponential it is possible to carry out a kinetic analysis of the quenching

process. As a further reasonable approximation the rates k_{11}, k_{22} and k_{21} may be considered as unimportant relative to the others enumerated above. The rate k_{1m} will also include any contributions from I* quenching by I_2 present as a residual impurity. The problem is now reduced to that of a kinetic scheme which has been extensively studied in the literature [13-15]. It can easily be shown that:

$$(p\tau_f)^{-1} \equiv \lambda_1 = k_e X_{O_2} + k_e' X_I + f[k_{12} X_{O_2} + k_{1m} X_m] \tag{21}$$

$$(p\tau_s)^{-1} \equiv \lambda_2 = (1-f) k_{1m} X_m + k_{12} X_{O_2} \tag{22}$$

where

$$f = k_e X_{O_2} / [k_e X_{O_2} + k_e' X_I]. \tag{23}$$

τ_f and τ_s are the lifetimes of the fast and slow decaying fluorescence components, respectively. Once the fluorescence decay is decomposed into the two components as shown in Fig. 9 we can also extract another valuable quantity - the relative fluorescence intensity of the short and long-lived components at time t=0. This intensity ratio is denoted as S. It can then further be shown that;

$$\frac{\lambda_1 + S\lambda_2}{1 + S} = k_e' X_I + k_{2m} X_m \tag{24}$$

$$\frac{\lambda_2 + S\lambda_1}{1 + S} = (k_e + k_{12}) X_{O_2} + k_{1m} X_m. \tag{25}$$

5.2 Evaluation of Rate Constants

Two sets of O_2 quenching data which have been reduced to be compatible with this analysis are tabulated in Table IV. We now have sufficient data to make an evaluation of the sum of rate constants ($k_e + k_{12}$) as defined in Eq. (25). Such a plot is shown in Fig. 10. The rate constant k_{1m} is the rate (or sum of rates) that was evaluated in section 3.1 for I* quenching by C_3F_7I (and residual I_2). Independent evaluations of k_{1m} were made on the particular sample of C_3F_7I used for a given O_2-I* quenching run since the purity of C_3F_7I subtly changed from day to day. It is possible to extract two further

TABLE IV

Quenching of $I(^2P_{1/2})$ in $n\text{-}C_3F_7I$ - O_2 Mixtures

Pressure C_3F_7I (torr)	Pressure O_2 (mtorr)	Molefraction $X(O_2) \times 10^{-3}$	Lifetime τ_f (usec)	Lifetime τ_s (usec)	Intercept Ratio (S)	$(p\tau_f)^{-1} \times 10^3$ $sec^{-1}\ torr^{-1}$	$(p\tau_s)^{-1} \times 10^3$ $sec^{-1}\ torr^{-1}$
25.0	0	0	-	220	-	-	0.182
25.4	20	0.79	39.4	109	1.8	1.00	0.36
25.5	40.7	1.60	25.2	121	5.5	1.56	0.32
25.2	60.1	2.38	16.0	112	6.9	2.47	0.35
25.2	80	3.16	13.8	122	9.2	2.86	0.32
25.4	99.3	3.89	10.6	102	9.6	3.70	0.38
25.2	119	4.70	9.3	101	10.3	4.25	0.39
50.1	0	0	-	160	-	-	0.125
48.9	50	1.02	18.2	65	1.8	1.12	0.31
47.6	93	1.95	11.6	67	4.0	1.81	0.31
50.3	123	2.44	8.5	84	10	2.33	0.24
50.6	150	2.95	6.6	42	5.3	2.98	0.47
51.0	200	3.92	5.5	50	8.0	3.56	0.39

rate expressions which are valuable in this analysis. It is easily shown that if $k_{2_m}X_m \ll k_{e'}X_I$ then,

$$\frac{\lambda_1 + S\lambda_2}{1 + S} = k_{e'}X_I, \tag{24}$$

$$k_e k_{e'} = \left[\frac{S}{(S + 1)^2}\right] \frac{(\lambda_1 + \lambda_2)^2}{X_I X_{O_2}} \tag{26}$$

and by combining and rearranging

$$k_e = \left[\frac{S}{(S + 1)}\right] \left[\frac{(\lambda_1 - \lambda_2)^2}{(\lambda_1 + S\lambda_2)}\right] \frac{1}{X_{O_2}} \tag{27}$$

The results of this analysis are shown in Fig. 11. The slope of the line in Fig. 11, then, gives a value for the rate k_e. From the data in Table IV and the plots in Fig. 9 and Fig. 10 and from other similar data and plots we arrive at a best value for the rates,

$$k_e = 0.96 \pm 0.12 \times 10^{-11} \text{ cm}^3\text{/molecule sec., and}$$

$$k_{12} = 1.42 \pm 0.11 \times 10^{-11} \text{ cm}^3\text{/molecule sec.}$$

The E-E transfer rate is reasonably consistent with that measured by other workers, i.e. $k_e = 0.93 \times 10^{-11}$ cm^3/molecule sec. by Donnovan and Husain [8], $k_e = 2.6 \times 10^{-11}$ by Deakin and Husain [6] and $k_e = 2.5 \times 10^{-11}$ cm^3/molecule sec by Burde and McFarlane [9]. However, none of the other authors have detected the second energy process which serves as an overall sink for I* atoms. One might argue that other workers have worked in an I* number density range up to 20 times less concentrated than in this work and that they missed the second decay component. The validity of this conjecture has yet to be deomonstrated.

5.3 Other Evaluations of k_{12}

Other workers have concluded that the k_{12} nonresonant quenching rate is much smaller than the number derived here. For example, Dervent and Thrush [16]

in an extensive analysis of I atom-O_2 kinetics conclude by indirect means that a value of $k_{12} = 4.5 \times 10^{-14}$ cm^3/molecule·sec is consistent with their overall kinetic analysis. They argue that a value very much larger would be entirely inconsistent with their data. Linevsky and Carbetta in a study of HI-O_2 kinetics in a fast flow reactor conclude after a kinetic analysis that their observations are consistent with a value for k_{12} which is ~140 times smaller than the value determined in this work. These observations would suggest that one needs to consider alternative explanations for the irreversable quenching mechanism.

5.4 Possible Alternative Kinetic Mechanisms

If one assumes that the alkyliodide quenching of $O_2(^1\Delta)$, k_{2m}, is an important rate and that $k_{12} \simeq 0$ then eq. (24-26) can be recast into appropriate form,

$$\frac{\lambda_2 + S\lambda_1}{1 + S} - k_1 m X_m = k_e X_{O_2}, \tag{25}$$

$$\frac{\lambda_1 + S\lambda_2}{1 + S} - k_{e'} X_I = k_{2m} X_m, \text{ and} \tag{24}$$

$$\frac{S}{(S + 1)^2} \quad \frac{(\lambda_1 - \lambda_2)}{k_e X_{O_2}} = k_{e'} X_I. \tag{26}$$

Carrying out the appropriate analysis then gives, $k_e = 0.96 \times 10^{-11}$ cm^3/molecule sec, as before, and $k_{2m} = 1.18 \times 10^{-14}$ cm^3/molecule sec. Independent evaluation of the C_3F_7I - O_2 ($^1\Delta$) quenching rate has not been carried out, however, typical quenching rates gathered from various sources for $O_2(^1\Delta)$ shown in Table V indicates that it is <u>very unlikely</u> that k_{2m} for C_3F_7I is 10^2 - 10^5 times larger than for other species.

TABLE V

$O_2(^1\Delta)$ Quenching Rates

Quencher	k_{2m}(cm^3/molecule sec)
CF_2Cl_2	4×10^{-19}
C_3H_8	2.5×10^{-18}
N atoms	2.8×10^{-16}
O atoms	$<1.3 \times 10^{-16}$

We have also considered other energy depletive routes such as the dimol reaction, the energy pooling reaction, and quenching by various radical products (i.e. C_3F_7, I atoms, etc.). Explanations involving any of the mechanisms considered in this section seem less plausible than the quenching mechanism explored in section 5.2. Never-the-less we are hesitant to strongly defend the assignment of the irreversable quenching rate to the oxygen quenching process, k_{12}.

6.0 TABULATION OF RATE DATA

The values which have been measured in this work for the bimolecular quenching rates of I ($^2P_{1/2}$) by various collision partners are presented in Table VI. Also presented are values measured by other workers for comparitive purposes.

7.0 SUGGESTIONS FOR FURTHER STUDIES

The observations in this work that an irreversable collisional quenching process involving O_2 and I* is taking place is of fundamental importance to the AFWL's efforts to produce a cw iodine laser. The implications are that this process must be detrimental to the effort to produce gain on this transition. It is disconcerting that we have not been able to absolutely assign the mechanism of this quenching process. However, no matter what the ultimate mechanism is proven to be, the quenching process is a harmful one to the cw I atom chemical laser. Hopefully, by better understanding the process it will be possible to adjust conditions such that the harmful process can be minimized. To do so will require a more firm understanding of the mechanism responsible for the quenching process.

Though further experiments are beyond the scope of this work we would like to suggest experiments of the following type which may be helpful in unraveling this complex process:

(1) Measurement of $I^* + O_2$ quenching rates as a function of laser power density. Such experiments will determine the importance of processes such as $I^* + I$, or $O_2(^1\Delta) + O_2(^1\Delta)$, or I* (or I) + $O_2(^1\Delta)$ all of which would be biphotonic in experiments such as these;

(2) Measurement of O_2 quenching rates as a function of total gas pressure. Such studies will evaluate the importance of three body processes such as $I^* + O_2 + M \rightarrow$ products or $C_3F_7\cdot + O_2 + M \rightarrow$ products, and;

(3) Measurement of O_2 - I* quenching rates using other I* precursors such as CH_3I, CF_3I or I_2. Such studies will determine the importance of the counter radical (i.e. $C_3F_7\cdot$, CH_3, I, etc.) in the quenching process.

TABLE VI

Bimolecular Quenching Rates of $I(^2P_{1/2})$

Quenching Partner	Rate (cm^3/molecule sec)	Other Values
C_3F_7I	$<2.5 \times 10^{-15}$	
H_2	0.85×10^{-13}	1.3×10^{-13} (a) 0.88×10^{-13} (b)
H_2O	3.75×10^{-12}	0.72×10^{-12} (a) 0.94×10^{-12} (b) 2.3×10^{-12} (c)
H_2O_2	4.04×10^{-11} (d)	1.0×10^{-11} (c)
$I^* + O_2(^3\Sigma) \rightarrow I + O_2(^1\Delta)$	$0.96 \pm 0.12 \times 10^{-11}$	2.6×10^{-11} (a) 0.93×10^{-11} (b) 2.5×10^{-11} (c)
$I^* + O_2(^3\Sigma) \rightarrow I + O_2(^3\Sigma)$	$1.42 \pm 0.11 \times 10^{-11}$ (c)	$<5 \times 10^{-14}$ (f) 0.9×10^{-13} (g)

References (a), see Ref.[6], (b) see Ref.[8], (c) see Ref.[9], (d) includes fast process only, (e) for explanation of this value see text, (f) see Ref. [16], (g) see Ref. [17].

8.0 REFERENCES

1 J. V. Kaspar, J. H. Parker and G. C. Pimentel, J. Chem. 43 1827(1965).

2 D. Husain and R. J. Donovan, Adv. in Photochem. 8 1(1972).

3a D. H. Burde, C. C. Davis and R. A. McFarlane, First Summer Colloquium on Electronic Transition Lasers, Santa Barbara, Ca., June (1974).

3b D. H. Burde, R. A. McFarlane and J. R. Wisenfeld, Chem. Phys. Letter 32 296(1975).

4a J. J. Deakin and D. Husain, J. Chem. Soc., Faraday Trans., II, 68 1603(1972).

4b J. J. Deakin, D. Husain and J. R. Wisenfeld, Chem. Phys. Letters 10 146(1971).

5 R. J. Donovan and D. Husain, Trans. Farad. Soc. 62 1050(1966).

6 J. J. Deakin and D. Husain, J. Chem. Soc., Faraday Trans., II, 68 41(1972).

7 T. Donohue and J. R. Wisenfeld, J. Chem. Phys. 63 3130(1975).

8 R. J. Donovan and D. Husain, Trans. Faraday Soc., 62 2023(1966).

9 D. H. Burde and R. A. McFarlane, J. Chem. Phys. 64 1850(1976).

10 J. J. Calvert and J. N. Pitts "Photochemistry," Wiley, New York 1966, p. 201.

11 H. E. Hunziker and H. R. Wendt, J. Chem. Phys. 60 4622(1974).

12 K. H. Becker, E. H. Fink, P. Langen and V. Schwarth, J. Chem. Phys. 60 4623(1974).

13 C. B. Moore, "Fluorescence," ed. G. Gailbault (Decker, New York, 1967), p. 174.

14 J. K. Hancock and W. H. Green, J. Chem. Phys. 57 4515(1972).

15 L. E. Brus and J. R. McDonald, J. Chem. Phys. 61 97(1974).

16 R. G. Derwent and B. A. Thrush, J. Chem. Soc., Faraday Disc., II, 53 162(1972).

17 M. J. Linevsky and R. A. Carabetta, "Chemical Laser Systems," ARPA Interim Technical Report, Contract #DAAH01-73-0653,(1974).

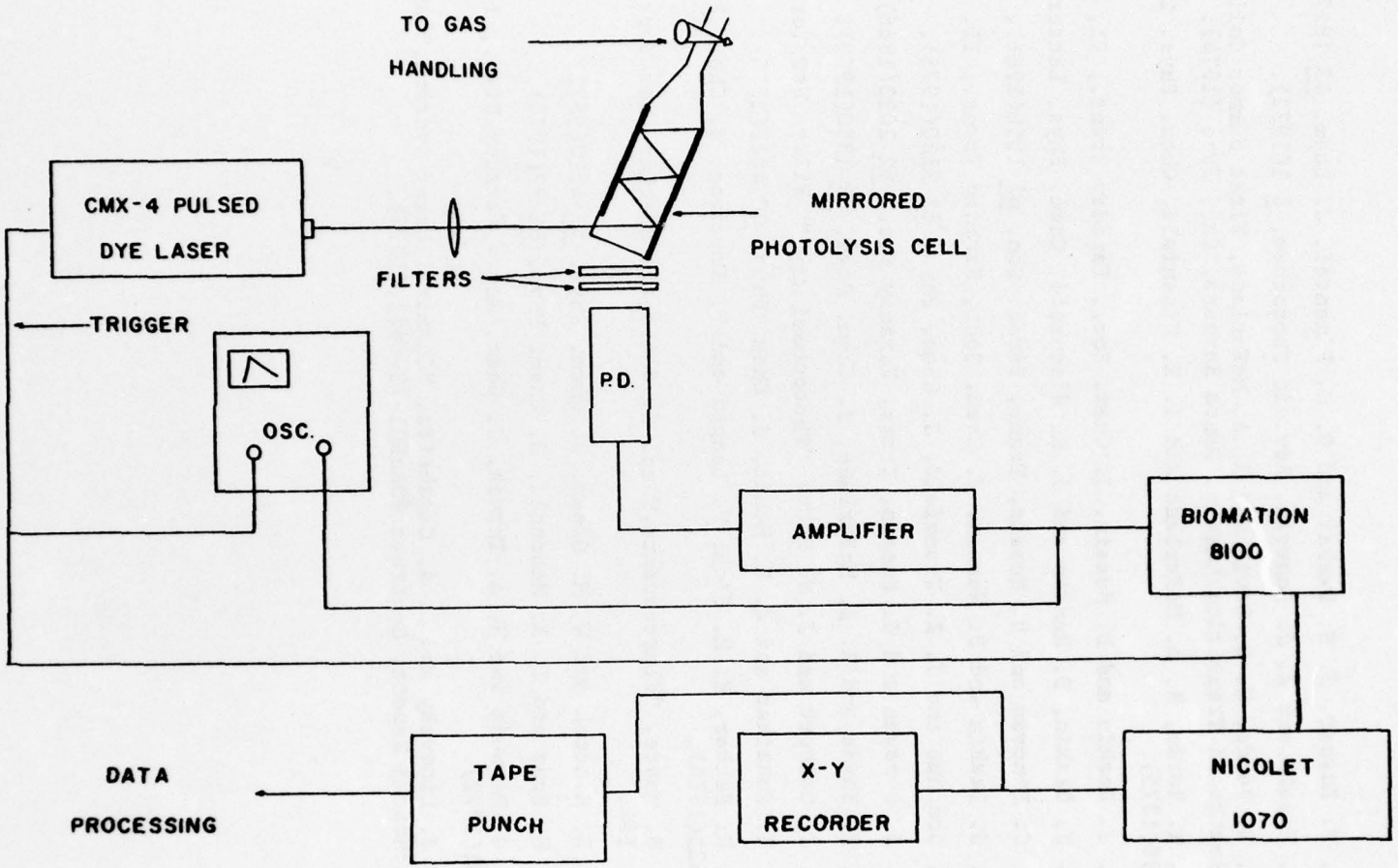

Fig. 1 — Fluorescence lifetime measuring apparatus

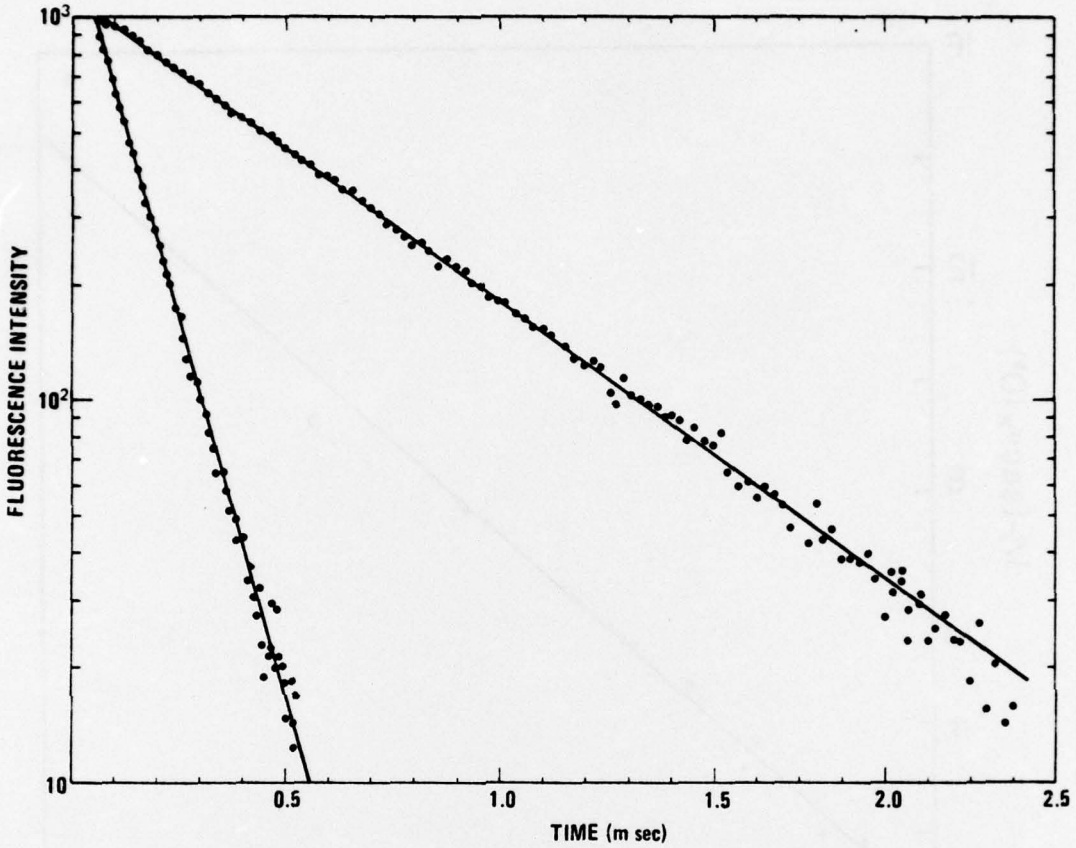

Fig. 2 — Semilog plot of I* fluorescence intensity. The plots demonstrate that the decay is completely single exponential over more than three fluorescence lifetimes. The C_3F_7I pressure in the upper curve is 11.9 torr while that in the lower curve is 49.5 torr.

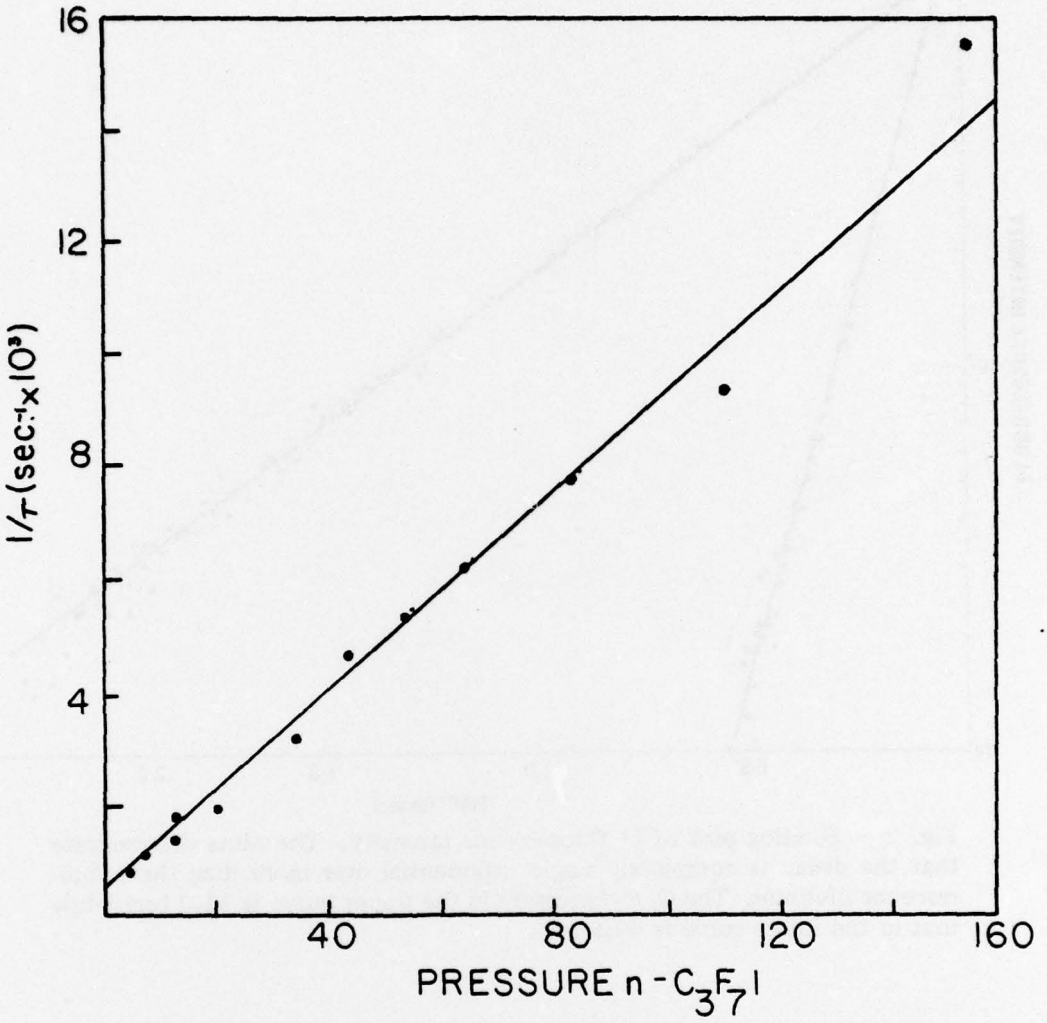

Fig. 3 — Stern-Volmer plot for I* atom quenching by n-C_3F_7I. The slope corresponds to an apparent quenching rate of ~100 sec^{-1}/torr.

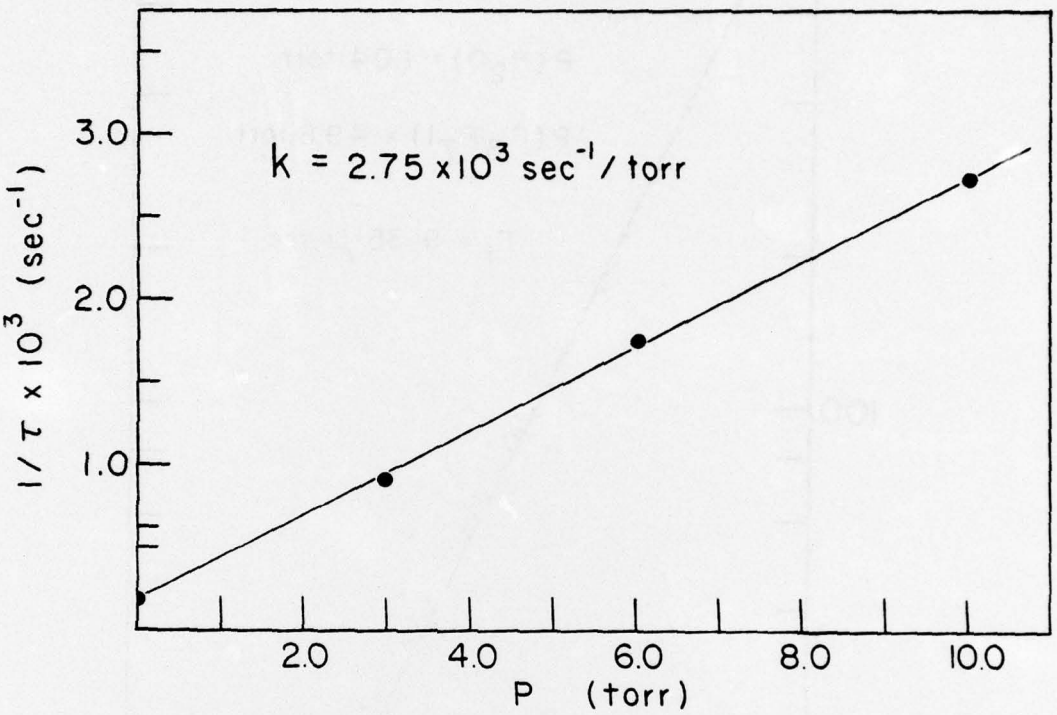

Fig. 4 — Stern-Volmer plot for I* atom quenching by H_2

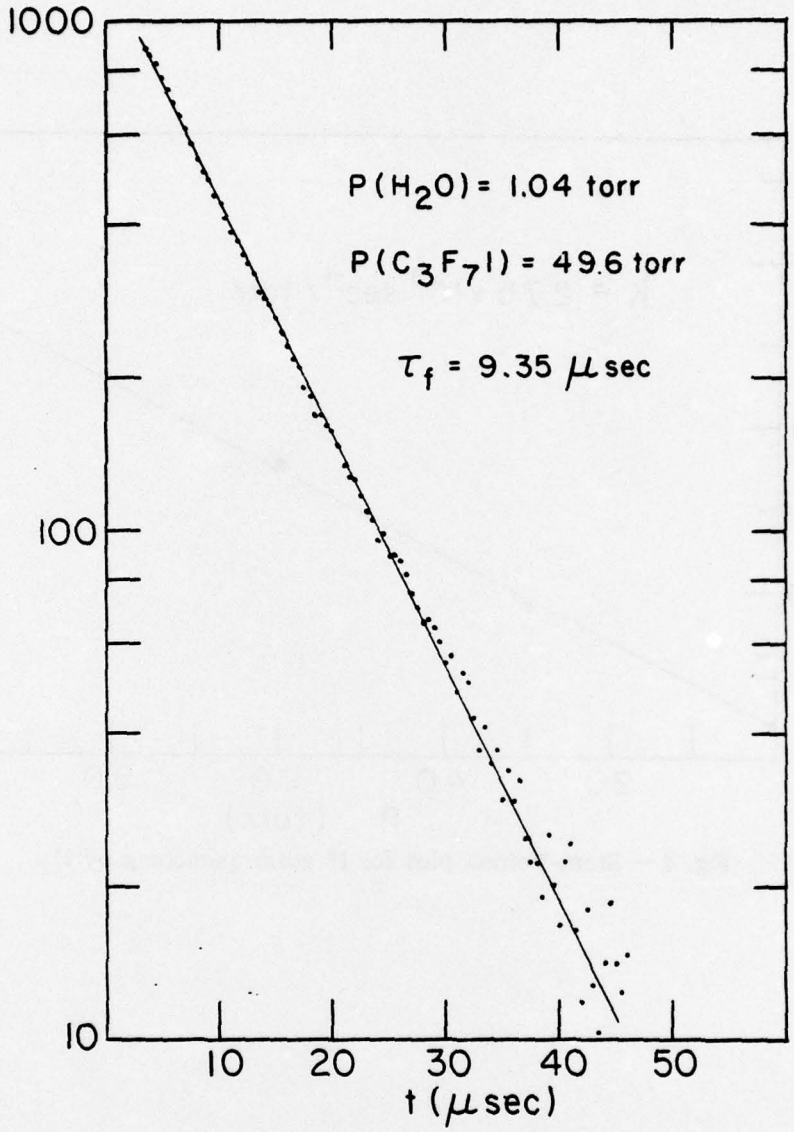

Fig. 5 — Semilog plot of I* fluorescence intensity in the presence of H_2O. The decay is clearly single exponential over three lifetimes.

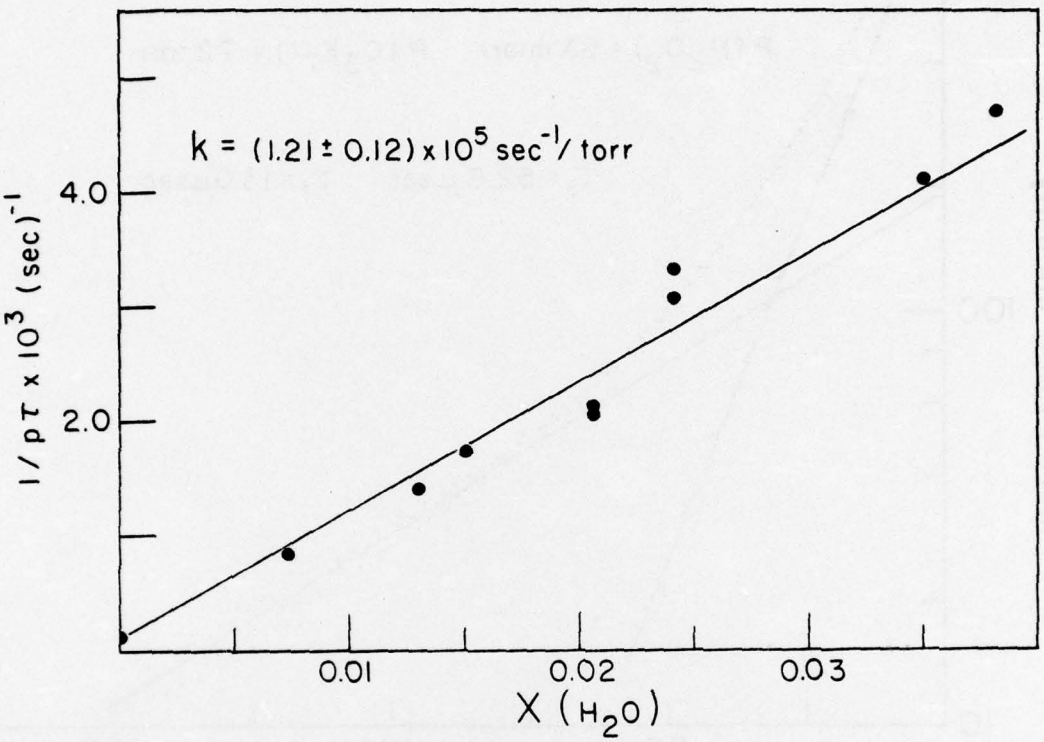

Fig. 6 — Stern-Volmer plot for I* quenching by H_2O

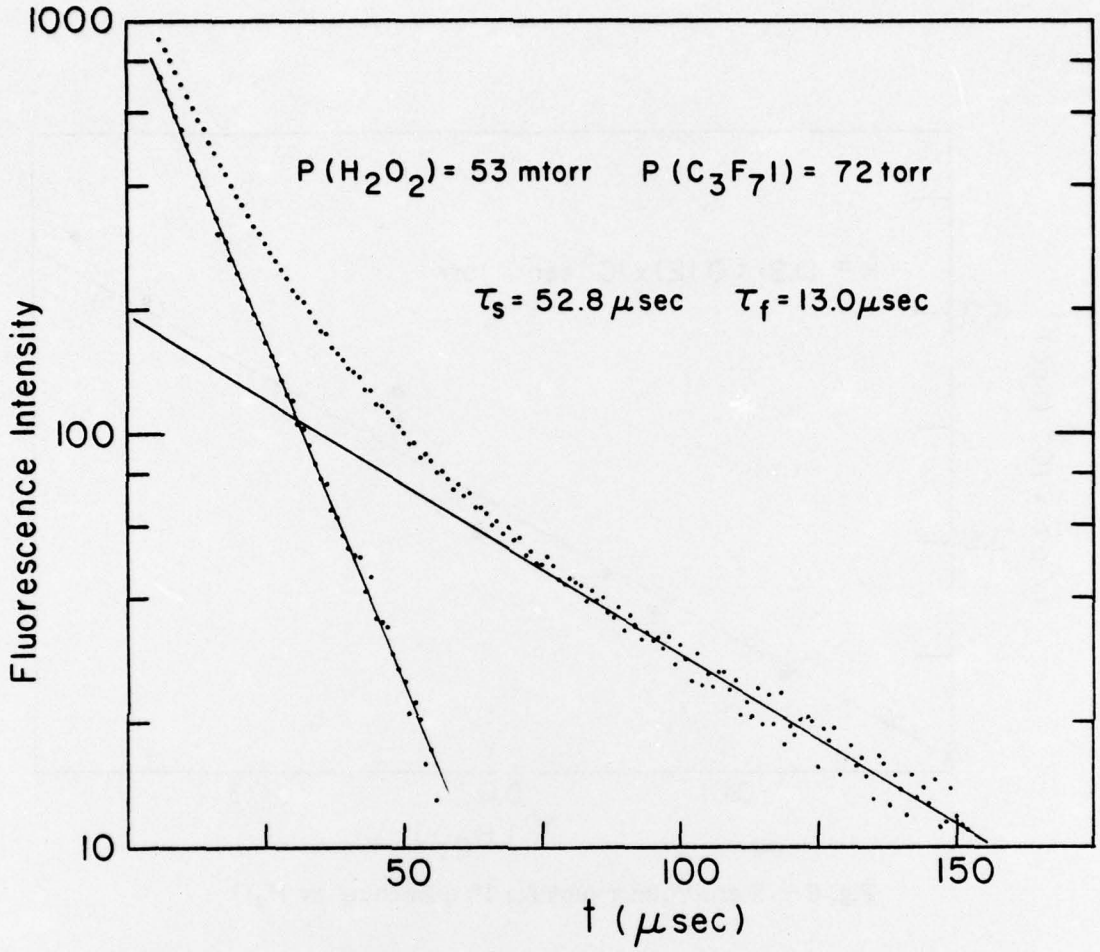

Fig. 7 — Semilog plot of fluorescence decay of I* in the presence of H_2O_2. The points on the upper curve are experimental data points. The lower set of data points is obtained by subtracting the exponential fit at long times from the experimental data points.

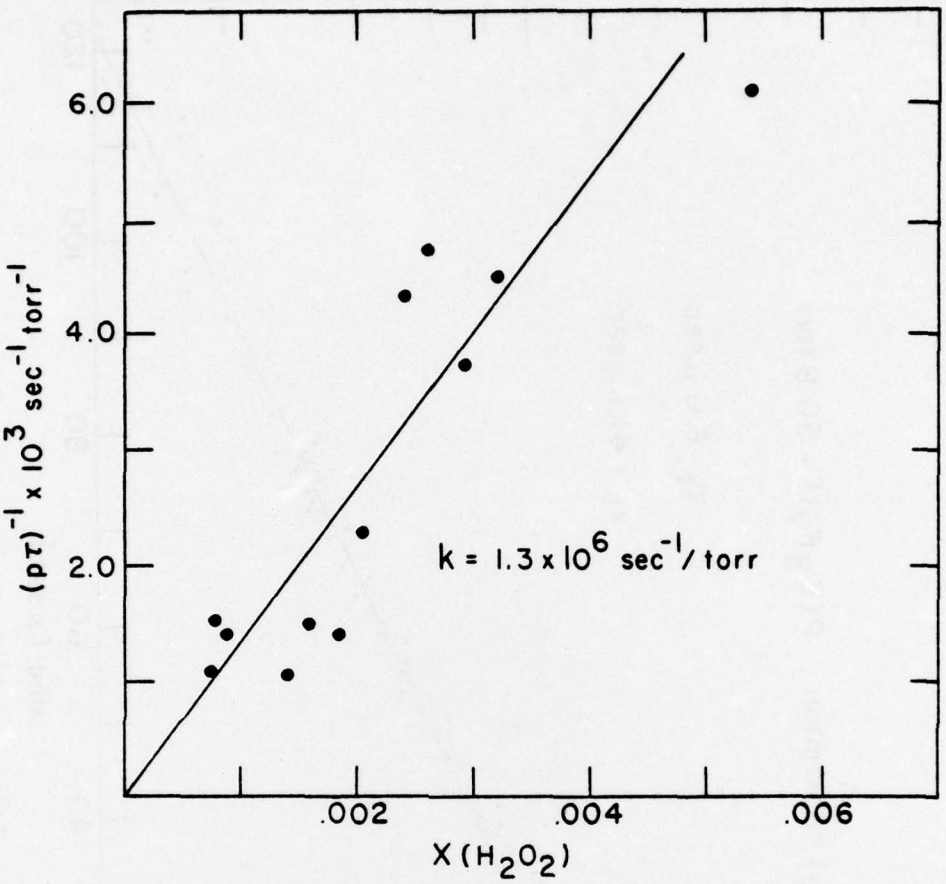

Fig. 8 — Stern-Volmer plot for I* quenching by H_2O_2. Data are evaluated from the fast decaying component only. See text for explanation.

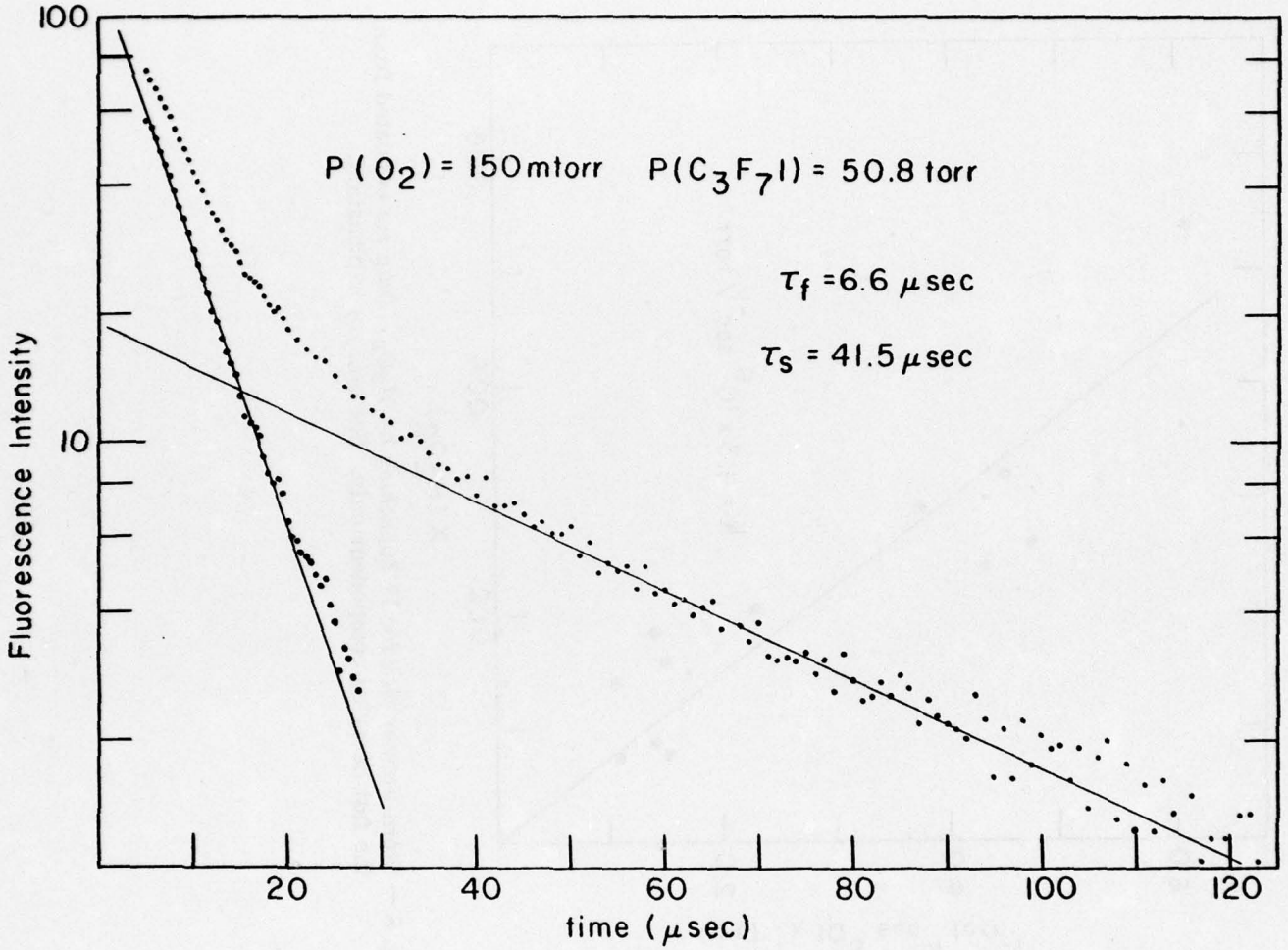

Fig. 9 — Semilog plot of biexponential fluorescence decay of I* in the presence of O_2. See caption of Fig. 7 for explanation.

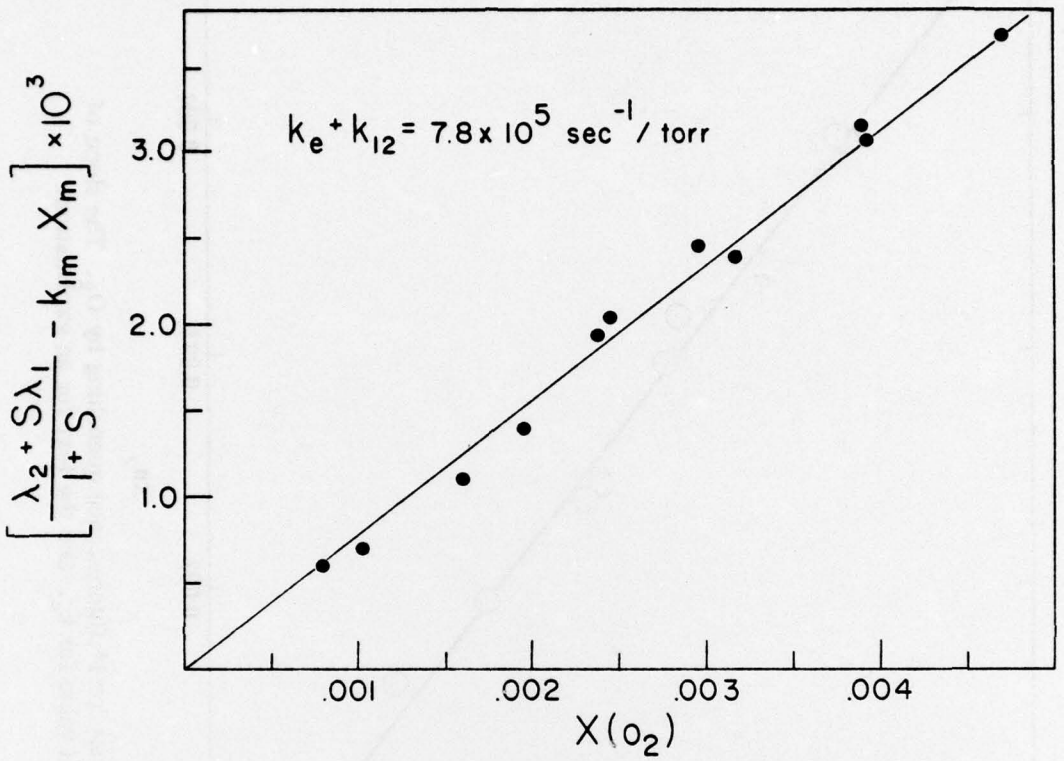

Fig. 10 — Kinetic analysis for I* fluorescence quenching by O_2. The slope of the curve gives a value for $k_e + k_{12}$. See the text for an explanation.

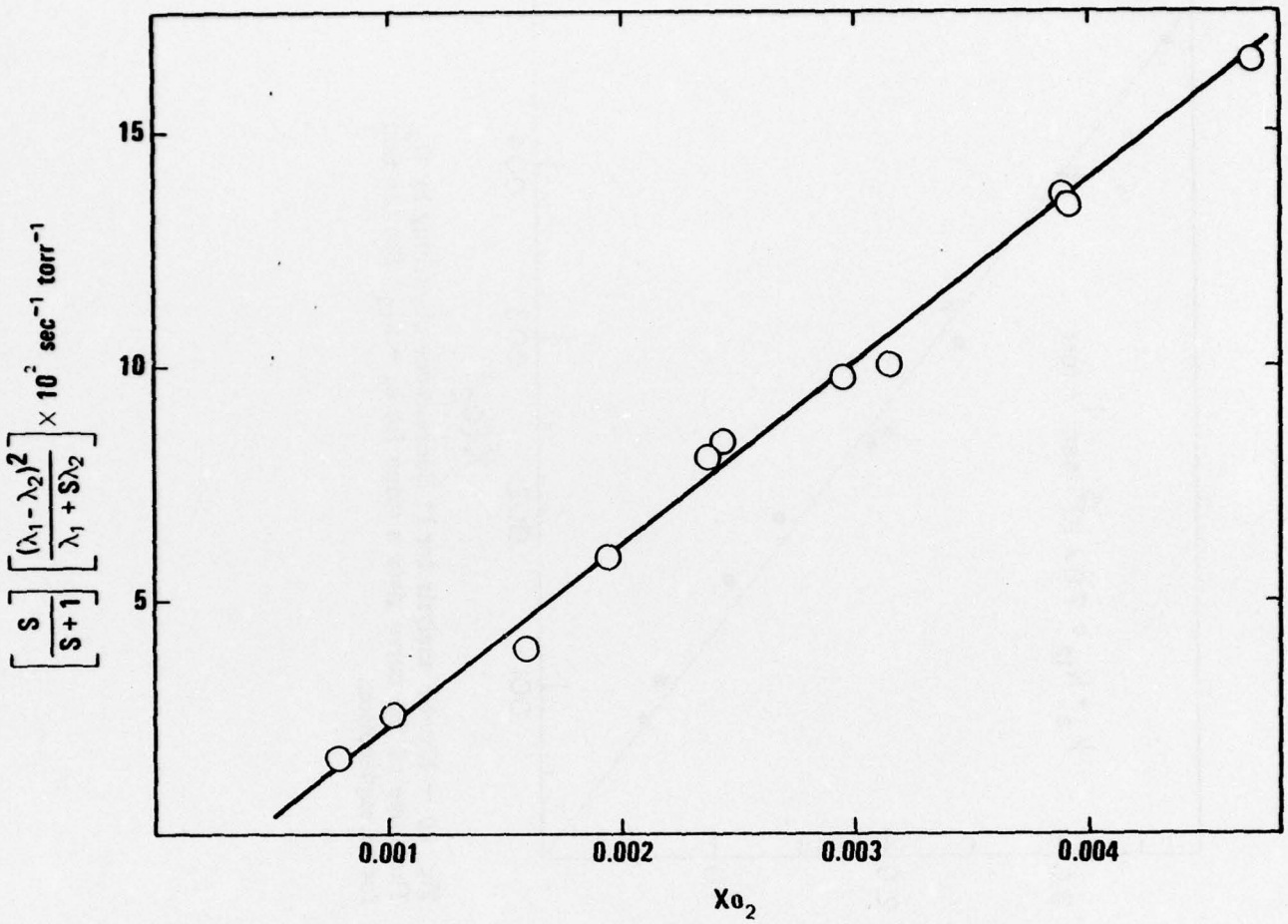

Fig. 11 — Kinetic analysis for I* fluorescence quenching by O_2. The slope of the curve gives a value for k_e. See the text for an explanation.